Biocatalysis and Agricultural Biotechnology 21 (2019) 101329

Contents lists available at ScienceDirect

Biocatalysis and Agricultural Biotechnology

journal homepage: http://www.elsevier.com/locate/bab

Response surface methodology and reaction optimization to product zero-valent iron nanoparticles for organic pollutant remediation

Raziyeh Kheshtzar [a], Aydin Berenjian [b,*], Narjes Ganji [c], Seyedeh-Masoumeh Taghizadeh [d], Mahmood Maleki [c], Saeed Taghizadeh [e], Younes Ghasemi [d], Ebrahiminezhad Alireza [f,**]

[a] Noncommunicable Diseases Research Center, Fasa University of Medical Sciences, Fasa, Iran
[b] School of Engineering, Faculty of Science and Engineering, The University of Waikato, Hamilton, New Zealand
[c] Department of Biotechnology, Institute of Environmental Sciences, Graduate University of Advanced Technology, Kerman, Iran
[d] Department of Pharmaceutical Biotechnology, School of Pharmacy and Pharmaceutical Sciences Research Center, Shiraz University of Medical Sciences, Shiraz, Iran
[e] Department of Medical Biotechnology, School of Advanced Medical Sciences and Technologies, Shiraz University of Medical Sciences, Shiraz, Iran
[f] Department of Medical Nanotechnology, School of Advanced Medical Sciences and Technologies, Shiraz University of Medical Sciences, Shiraz, Iran

ARTICLE INFO

Keywords:
Bioreduction
Biosynthesis
Design of experiments (DoE)
Dye removal
Fenton-like catalysts
Plant mediated synthesis

ABSTRACT

Zero-valent metals such as Al^0, Zn^0, Ti^0, and Fe^0 with well explored catalytic activity have gained wide spread applications in the remediation proposes. Due to extremely high surface to volume ratio, nanoscale zero-valent metals showed increased catalytic potential and introduced as promising catalysts. Among zero-valent metal nanoparticles, zero-valent iron nanoparticles (ZVINPs) are one of the most employed nanostructures in remediation studies. These particles are effective Fenton-like catalysts and employed to remove organic contaminations. Recent studies indicated that plant mediated synthesized ZVINPs are more efficient in this regard than chemically synthesized nanoparticles. The extract of green tea is extensively used for green synthesis of various metallic nanoparticles and iron based nanoparticles. In the present work, design of experiments (DoE) and response surface methodology (RSM) was applied to find out effective reaction parameters and optimal reaction condition for maximum production of ZVINPs by using green tea extract. For this purpose, at first, a fractional factorial design was used to screen the reaction parameters (reaction time, temperature, amount of leaf extract, and metal precursor concentration) in the synthesis process. Subsequently, the central composite face (CCF) design was utilized for reaction optimization. Amount of green tea extract and iron precursor concentration were found to be the most effective parameters. In a regular 10 mL reaction, maximum productivity was achieved by employing 9 mL tea extract and 25 mM (final concentration) ferric chloride. The prepared nanoparticles were identified to be amorphous ZVINPs with a low magnetization value of 80 memu/g. The particles diameter was measured to be 5–20 nm with 11.2 nm mean size. The particles pose effective catalytic activity for organic contaminants removal. Methyl orange was tested as a common model compound and particles were capable to eliminate more than 50% of the initial dye in just 2 h.

1. Introduction

Azo dyes are commercially abundant family of azo compounds. These compounds are organic chemicals with diazenyl (R–N=N–R′) functionality. Azo dyes have gained diverse applications in various industries such as food, leader, and textile industries. Due to their widespread applications, azo dyes and azo compound derivatives are considered as one of the important aquatic contaminants (Tatarko et al., 1999; Gudelj et al., 2011). Intense industrial activities and production of wastewaters with a very complex content increases demand for new treatment technologies (Khoo et al., 2019). Environmental nanotechnology and application of nano size materials for high efficient remediation is one of these new technologies (Lahann, 2008). Nanostructures of zero-valent metals such as Al^0, Zn^0, Ti^0, and Fe^0 are promising compounds in this regard (Lu et al., 2016; Yang et al., 2019). Zero-valent iron nanoparticles (ZVINPs) due to strong adsorption capability, high

* Corresponding author.
** Corresponding author. Unit 23, Floor 2, School of Advanced Medical Sciences and Technologies, Almas Building, Mulla Sadra Intersection, Shiraz, 71336-54361, Iran.
E-mail addresses: aydin.berenjian@waikato.ac.nz (A. Berenjian), a_ebrahimi@sums.ac.ir (A. Ebrahiminezhad).

https://doi.org/10.1016/j.bcab.2019.101329
Received 27 June 2019; Received in revised form 28 August 2019; Accepted 2 September 2019
Available online 3 September 2019
1878-8181/

reducibility and potent catalytic activity are the most studied and employed nanostructures in novel remediation approaches. These particles exhibit a potent activity to treat organic contaminations in water and wastewater at ambient atmosphere (Ebrahiminezhad et al., 2017c; Taghizadeh et al., 2019). It is believed that ZVINPs do not simply act as an adsorbent or a reducer. It acts through sequential or simultaneous complex processes (*e.g.* adsorption, reduction, dissolution, and precipitation) that occur on the surface of nanoparticles. ZVINPs alone can act as reducing agent, but, in the presence of oxygen compounds such as water and hydrogen peroxide ZVINPs efficiently produce reactive oxygen species (ROS). These free radicals are responsible in the degradation of organic contaminants (Rezaei and Vione, 2018). Production of ROS is due to release of ferrous ions from ZVINPs. Surface of these particles is usually oxidized in aerated environments and iron ions are released from the oxide coating. Increase in the surface area provides more space for oxidation and iron ions release (Li et al., 2006; Torrey et al., 2015; Rezaei and Vione, 2018).

The widespread applications of ZVINPs encourage researchers to employ different physical and chemical methods such as ball milling, ion sputtering, sol-gel synthesis, chemical vapor deposition, spark discharge, and aqueous phase reduction for the fabrication of these nanostructures (Li et al., 2016; Seifan et al., 2019). Reduction of iron ions with powerful chemical reductants such as sodium borohydride ($NaBH_4$) is one of the most common techniques in this regard (Yuvakkumar et al., 2011; Akbari and Mohamadzadeh, 2012). But, there are major drawbacks with these methods such as harsh reaction condition and employing toxic chemicals and organic solvents that make the process unsustainable (Yuvakkumar et al., 2011; Akbari and Mohamadzadeh, 2012). To overcome the adverse effects and intrinsic limitations of conventional synthesis methods, researchers have explored green synthesis as an economic and sustainable technique (Machado et al., 2013; Ebrahiminezhad et al., 2017b). In this modern alternative, biologic compounds from living organisms such as plants, microbes, and algae have been used for the reduction of iron ions to ZVINPs (Ebrahiminezhad et al., 2016a, 2017d; Kianpour et al., 2016, 2018). Nowadays, green synthesis attracts a lot of attention and became a promising approach toward elimination of organic solvents and toxic chemicals from synthesis reactions (Kumar and Singhal, 2007; Sulaiman et al., 2018). Behind all beneficial aspects of green synthesis, there are some restricting parameters with employing microbial cells including difficulty of handling, slow reaction time, contamination concerns, and being less economic (Ghasemi et al., 2011; Ebrahiminezhad et al., 2014b). But, plants mediated synthesis can prevail over other biological processes because it eliminates the elaborate process of cell culture and cell storage and can also be scaled up for large-scale productions. From environmental nanotechnology point of view it has been shown that green synthesized nanoparticles are more efficient in remediation studies than chemically synthesized particles (Muthukumar and Matheswaran, 2015). It is claimed that better catalytic activity of green synthesized nanoparticles is mainly due to biologic coating that occur through green synthesis. This effective coating prevents particles aggregation and provides larger surface area (Muthukumar and Matheswaran, 2015).

Plants are abundant with organic compounds such as polyphenols, flavonoids, proteins, reducing sugars, nitrogen bases, and amino acids that can act as reducing and capping agent for the synthesis of iron nanoparticles (Ebrahiminezhad et al., 2016b, Ebrahiminezhad et al., 2017; Yew et al., 2019). Since now, a variety of plants such as *Lantana camara*, *Annona squamosal*, *Anacardium occidentale*, *Urtica dioica*, *Cupressus sempervirens*, *Psoralea corylifolia* seeds, *Eucalyptus globulus*, and so forth have been used successfully to produce iron based nanoparticles (Tucek et al., 2010; Tuček et al., 2015; Ebrahiminezhad et al., 2017a, 2017b; Nagajyothi et al., 2017). Green tea is a type of tea that produced from *Camellia sinensis* leaves and frequently was employed for the green synthesis of iron and other metallic nanoparticles (Wang et al., 2014b; López-Sánchez et al., 2016; Ohkoshi et al., 2016; Truskewycz et al., 2016). It belong to the genus *Camellia* of flowering plants in the *Theaceae* family. *C. sinensis* originated in Southeast Asia such as China and India, but, presently is cultivated in many countries (Grundl and Delwiche, 1993). Numerous studies have shown that the consumption of green tea provides health benefits against cardiovascular disease, glycaemia, hyperlipidemia, inflammation, obesity, and cancer (Yuvakkumar et al., 2011; Li et al., 2016; Jiang et al., 2018). Green tea extract is rich of phytochemicals such as polyphenols, carbohydrates, flavonoids, proteins, and vitamins that play a key role in the reduction and synthesis of metallic nanoparticles (Grundl and Delwiche, 1993). So, green tea extract is now known as one of the first choices for the green synthesis of ZVINPs and other metallic nanoparticles (Huang et al., 2014a; Huang et al., 2014b, Plachtová et al., 2018).

Behind potential of the employed plant for the synthesis of nanoparticles various parameters such as reaction time, reaction temperature, amount of leaf extract, and metal precursor concentration are other key parameters in the green synthesis of iron nanoparticles (Ebrahiminezhad et al., 2016b, 2016c). Nevertheless, to date very rare studies have been done to find out the effective factors in the biosynthesis of iron based nanoparticles, interaction of different factor, and optimal reaction condition (Borja et al., 2015). On the other hand, almost all previous investigations in this regard were performed based on the preliminary methods such as one-factor-at-a-time experiment (Ebrahiminezhad et al., 2016b, 2016c). This method cannot describe interactions among the various parameters which involved in the synthesis process. Meanwhile, knowledge about the effective parameters and their interactions is the key element to achieve an optimal point in production of any material. So, the conduction of statistical optimization studies is mandatory for green construction and employment of ZVINPs as a novel catalyst for environmental remediation proposes. Consequently, effective parameters, their interactions, and optimal reaction condition were explored for the green fabrication of ZVINPs using green tea extract. Design of experiments (DoE) and response surface methodology (RSM) were carried out to achieve maximum production of nanoparticles (Berenjian et al., 2011; Ghoshoon et al., 2015; Ranmadugala et al., 2017). Finally, the catalytic potential of the prepared nanoparticles was examined to remove azo dyes.

2. Materials and methods

2.1. Materials

Dried leaves of green tea were purchased from a local shop. Ferric chloride ($FeCl_3{\cdot}6H_2O$) was purchased from Merck Chemicals (Darmstadt, Hessen, Germany) and used directly without refinement. Laboratory glass-wares were washed with acid solution and deionized water. Millipore water (Millipore Corp., Bedford, MA, USA, conductivity range of 0.055 − 0.294 lS/cm) was used for all synthesis reactions and leaves extraction.

2.2. Leaves extract preparation

Green tea leaves were milled with a household miller (Parskhazar, Model Chili, Iran) and passed through a sieve with particular mesh size. For leaves extraction, 5 g of leaves powder was mixed with 100 mL deionized water in a 250 mL round bottom flask (Nagajyothi et al., 2017; Rajiv et al., 2017). The mixture was boiled (at about 97 °C) for 15 min by using a heater mantel and under reflux. Resultant extract was cooled down to room temperature and filtered through a Whatman paper (Reeve angel, Grade 201) to remove the sludge. Then the filtrate was centrifuged (4200 g, 12 min) to remove fine leaf particles. Therefore, a clear supernatant was obtained and used for further experiments.

2.3. Experimental design

The statistical design of experiments using Modde software version 9

(Umetrics, Sweden) was employed to identify the factors which have the most significant effects on the maximizing the production of INPs. On the other hand, this screening was used to find out which factors are the dominating ones and to find out the optimal ranges in the synthesis process. In the first step, the important factors with significant effects on the amount of synthesized nanoparticles were specified. For this reason, a fractional factorial design was utilized to screen the effect of four variables including of green tea extract quantity, iron precursor concentration, reaction temperature, and reaction time.

The aim of the second step was to achieve an empirical model of optimization process to determine the optimum concentrations of selected efficient factors. In this step, RSM with central composite face (CCF) design was employed to optimize the effective factors chosen from screening stage on the green synthesis productivity. The variables and their real values used in the CCF design are represented in Table 1.

2.4. Synthesis of iron nanoparticles

Synthesis of INPs with maximum productivity was conducted based on the optimization data and the reaction was performed in 10 mL final volume as following. Leaves extract (9 mL) and deionized water (750 μL) were added to a 50 mL round bottom flask and stirred vigorously at room temperature. Synthesis reaction was started by injection of 250 μL iron precursor (FeCl3·6H2O, 1 M) in to the flask and reaction was followed for 15 min. Then the reaction mixture was centrifuged and the resulting black pellet was washed with distilled water for three times to remove unreacted solutes and phytochemicals. Finally, black precipitate was dried in an oven at 50 °C for 48 h and characterized as follow.

2.5. Characterization of iron nanoparticles

Transmission electron microscopy (TEM, Zeiss, EM900, HT-100 KV) was performed for characterizing size and shape of the synthesized iron nanoparticles. For these measurements, a drop of particles suspension was loaded on a carbon-coated copper grid and was allowed to dry at room temperature. Micrographs were taken without any more sample preparation and particle size analysis was conducted by using an image analysis software (ImageJ version 1.47v, developed by NIH, http://imagejnihgov/ij/). Fourier-transform infrared (FTIR) spectroscopy (PerkinElmer Spectrum One) analysis was done using KBr pellets for understanding the existence of surface functional groups on the nanoparticles. The IR absorption analysis was done from 4500 cm^{-1} to 400 cm^{-1} at room condition (Ebrahiminezhad et al., 2014a, 2016a). The crystal structure of synthesized nanoparticles was studied with an x-ray diffractometer (Siemens D5000). X-ray diffraction (XRD) pattern was evaluated using X'Pert HighScore version 1.0d (PAN analytical B·V., Almelo, the Netherlands). Vibrating sample magnetometer (VSM) was employed for magnetic evaluations of the obtained nanoparticles at room temperature (American-Lake Shore Cryotronics company, 7407 Model). Thermogravimetric analysis (TGA, 209 F3Tarsus) was performed to evaluate the thermal stability and quantification of organic compounds from green tea extract in final INPs product. Thermogravimetric analysis (TGA) and derivative thermogravimetric (DTG) analyses were performed with 10 °C/min heating rate, from 30 to 600 °C, under ambient atmosphere.

Table 1
Experimental design and results of screening factors affecting green synthesis of INPs.

Run	Experimental factors				Response
	$FeCl_3$(mM)	Leaf extract (mL)	Temperature (°C)	Time (h)	Weight (g)
1	1	1	25	0.25	0.0051
2	100	1	25	0.25	0
3	1	9	25	0.25	0
4	100	9	25	0.25	0.0174
5	1	1	75	0.25	0
6	100	1	75	0.25	0.001
7	1	9	75	0.25	0
8	100	9	75	0.25	0.0421
9	1	1	25	24	0
10	100	1	25	24	0.0028
11	1	9	25	24	0.0017
12	100	9	25	24	0.0481
13	1	1	75	24	0.0018
14	100	1	75	24	0.0038
15	1	9	75	24	0.0029
16	100	9	75	24	0.054
17	50.5	5	50	12.125	0.0275
18	50.5	5	50	12.125	0.0263
19	50.5	5	50	12.125	0.0255

2.6. Catalytic activity assay

Methyl orange is a common model compound to evaluate the catalytic power of Fenton-like catalysts and employed in diverse environmental studies (Shahwan et al., 2011; Muthukumar and Matheswaran, 2015; Youssef et al., 2016; Xu et al., 2018; Taghizadeh et al., 2019). Hence, in this experiment a methyl orange degradation reaction was set to investigate the catalytic potency of the prepared nanoparticles. The reaction parameters were set based on the previous reports (Youssef et al., 2016; Taghizadeh et al., 2019). In brief, nanoparticles were exposed to Methyl orange dye solution (20 mg/L final concentration) with hydrogen peroxide (1% V/V). The dye degradation rate was followed for 6 h via colorimetric assay (Agilent technologies Cary Series UV/VIS) at 465 nm using methyl orange standard curve.

2.7. Statistical analysis

One-way Analysis of Variance (ANOVA) with post-hoc mean comparison with Tukey test was used to evaluate the experimental data with the statistical significance level of $p < 0.05$.

3. Results and discussion

3.1. Impacts of different factors on the nanoparticles production

In the first step, a combination of various factors was used to investigate the significant factors and their interaction on nanoparticles production. Based on previous investigations, reaction time, iron precursor concentration, leaves extract quantity, and reaction temperature were set as potential parameters. DoE was carried out base on these four parameters and amount of produced nanoparticles in each experiment utilized in screening the RSM (Berenjian et al., 2011). Table 1 gives the combination of variables used in experimental design and depicted the results of initial screening for effective factors in the synthesis reaction. Statistical analysis of data is presented in Table 2 to illustrate the main effects of single parameters and their interactions on the weight of produced nanoparticles (Ranmadugala et al., 2017). Based on these result, the low *P*-value ($P < 0.05$) for iron precursor concentration and leaves extract reveals that they are the effective factors for synthesis of INPs using green tea extract. Coefficient for these two variables showed their positive effect on the response. These findings are in close agreement with previous studies on the synthesis of iron nanoparticles using green tea extract. Where, authors demonstrated a dependency between $FeCl_3$-to-green tea extract ratio and amount of nanoparticles formation (Borja et al., 2015).

3.2. Optimization of iron nanoparticles production

From the screening data, it can be concluded that the key parameters which affecting the synthesis reaction are iron precursor concentration and amount of green tea extract (Table 1). Therefore, these two ingredients were chosen to further examine the optimal production of INPs

Table 2
Statistical analysis and coefficients of the variables for optimal reaction condition to green synthesis of INPs.

Terms	Coefficient	Std. Err.*	P-value
Constant	0.013	0.002	0.000
X_1	0.009	0.002	0.003
X_2	0.009	0.002	0.004
X_3	0.001	0.002	0.457
X_4	0.003	0.002	0.240
X_1. X_2	0.009	0.002	0.003
X_1. X_3	0.002	0.002	0.400
X_1. X_4	0.002	0.002	0.264
X_2. X_3	0.002	0.002	0.421
X_2. X_4	0.002	0.002	0.283
X_3. X_4	−0.000	0.002	0.791

* Std. Err. = standard error, $X_1 = FeCl_3$, X_2 = Leaf extract, X_3 = Temperature, X_4 = Time, $R^2 = 0.871$ and R^2 (adj.) = 0.709.

through RSM. To achieve more sustainable reaction condition with less energy consumption, the reaction temperature was let to be ambient temperature for all optimization experiments and reactions were carried out in minimum time (15 min). Determination of optimum values for key factors to enhance the INPs production was performed using the central composite face (CCF) design as shown in Table 3. The results of ANOVA test with the model F value of 14.4367 and probability value of 0.005 indicates a good fitness of the model (Table 4). Also the linear regression coefficient $R^2 = 0.935$ and the adjusted determination coefficient R^2 of 0.870 demonstrate the adequacy of the model.

Fig. 1 illustrates the response surface plots of INPs production for the effects of key factors. The plots demonstrate that the highest amount of INPs is achievable when the iron precursor concentration and tea extract are set as 25–35 mM and 8.5–9 mL, respectively. As can be seen in Fig. 1, fabrication of nanoparticles decreases when the values of iron precursor concentration and amount of green tea extract are set to be more than 35 mM and less than 8.5 mL, respectively. The developed model predicted that highest productivity to be 22 mg per reaction (2.2 mg per mL of the reaction mixture) with optimum values of iron precursor (25 mM) and green tea extract (9 mL). Consequently, the validity of experiment was confirmed under the optimized condition where, observed value was the production of 0.019 g/mL INPs.

Experimental evidences showed that synthesis condition has a great impact on the physical and chemical properties of the biosynthesized nanoparticles (Ebrahiminezhad et al., 2016b, 2016c, 2017c. Consequently, with regard to notability of reaction conditions and important factors in green synthesis processes, more studies must be done to determine their impacts on reactivity and physicochemical properties of the synthesized nanoparticles. For instance, Lanlan Huang reported that the reactivity of the prepared nanoparticles was extremely depended to the synthesis conditions and involved parameters (such as the ratio of iron precursor (Fe^{2+}) and leaf extract (tea extract), reaction temperature, and pH (Huang et al., 2015).

Table 3
Central composite face design matrix for the significant variables and observed response.

Run	Experimental factors		Response
	$FeCl_3$ (mM)	Leaf extract (mL)	Weight (g)
1	25	5	0.0117
2	75	5	0.0024
3	25	9	0.0199
4	75	9	0.0189
5	25	7	0.0166
6	75	7	0.005
7	50	5	0.0009
8	50	9	0.0206
9	50	7	0.0074
10	50	7	0.0062
11	50	7	0.0075

Table 4
Analysis of variance for the fitted quadratic model.

Source of Variation	DF*	SS*	MS(variance)*	*F* value	*P* value	SD*
Total	11	0.001	0.000			
Constant	1	0.001	0.001			
Total corrected	10	0.000	5.244			0.007
Regression	5	0.000	9.809	14.4367	**0.005**	0.009
Residual	5	3.397	6.795			0.002
Lack of Fit	3	3.292	1.097	20.9737	**0.046**	0.003
Pure error	2	1.046	5.233			0.000

* DF: degree of freedom, SS: sum of squares, MS: mean sum of squares, SD: standard deviation.

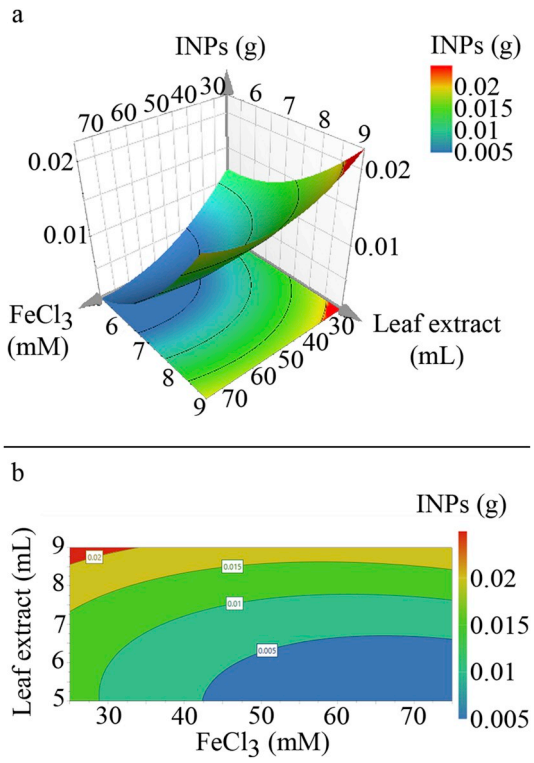

Fig. 1. Response surface plot (a) and response counter plot (b) for the fabrication of INPs showing the effects of iron precursor concentration and amount of leaf extract in a green synthesis reaction, all reactions were done in 10 mL final volume. (For interpretation of the references to color in this figure legend, the reader is referred to the Web version of this article.)

3.3. Synthesis of INPs

Optimum concentration of significant factors that obtained from optimization process were used in green synthesis of INPs using green tea extract. The optimal synthesis reaction was carried out by addition of iron precursor to the leaf extract. A rapid color change in the reaction and create a dark black suspension indicates formation of INPs and reduction of iron ions to INPs. This phenotypic change also indicates the high reduction potential of phytochemicals in the green tea extract (Ebrahiminezhad et al., 2017a, 2017b).

3.4. Characterization of iron nanoparticles

3.4.1. Transmission electron microscopy

TEM analysis of iron nanoparticles confirmed the successful synthesis of iron nanoparticles from green tea extract. TEM images of INPs

and corresponding size distribution histogram are presented in Fig. 2. Results showed that the majority of particles possess a spherical morphology, but, some rare truncated triangular, ellipsoidal, drop shape, and polyhedral particles were also observed. Similar morphology has been reported by other researchers for the green tea mediated synthesized zero-valent INPs (Borja et al., 2015).

The particles diameter was measured to be 5–20 nm with 11.2 nm mean size. In contrast to previous reports for the synthesis of INPs using green tea, reaction optimization resulted in smaller particles. In these experiments, the size range from 20 nm to 80 nm have been reported (Kuang et al., 2013; Wang et al., 2014a, 2014b; Huang et al., 2015; Truskewycz et al., 2016). The other advantage of the prepared particles over previous reports is that in previous experiments resulted nanoparticles were entrapped in plant organic compounds and form macro scale aggregated structures (Shahwan et al., 2011). But, no macrostructure was observed in the current experiment. Feature improvements for the prepared nanoparticles can be due to reaction optimization. It is obvious that reaction condition has an immense effect on the resulted nanoparticles characteristics (Karade et al., 2018).

3.4.2. Fourier-transform infrared spectroscopy

FTIR analysis was conducted to understand the chemical composition of the green synthesized ZVINPs, and phytochemicals that are responsible for synthesis, capping and stabilizing of nanoparticles. As shown in Fig. 3, peaks and corresponding bond identities were identified as follow. The peak at 3393 cm^{-1} is indicative of O-H stretching vibrations. The peak at 2918 cm^{-1} corresponds to C-H and CH_2 vibration of aliphatic hydrocarbons. C═C aromatic ring stretching vibrations produced a peak at 1630 cm^{-1}. C-N stretching vibration from aromatic amines absorbed IR at 1367 cm^{-1}. The peak at 1212 cm^{-1} is a marker for phenolic C-O stretching, and peak at 1031 cm^{-1} describes C-O stretching for the OH substituent of the pyran ring (Wang et al., 2014a; Truskewycz et al., 2016; Xiao et al., 2016). These functional groups indicate the presence of bioactive compounds in the green tea extract that act as

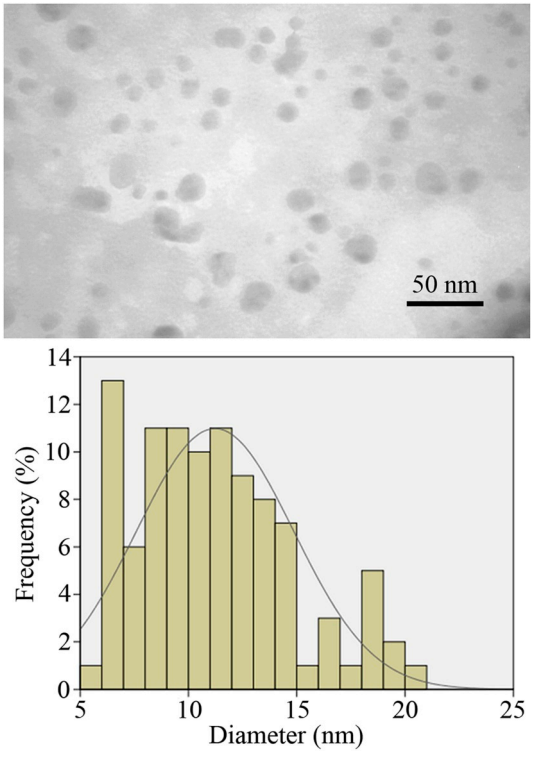

Fig. 2. TEM micrograph of the biosynthesized INPs (a), which indicates that nanoparticles are spherical in shape, and corresponding particle size distribution histogram (b).

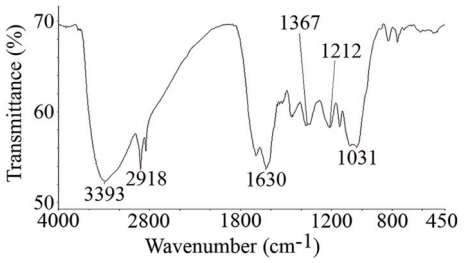

Fig. 3. Fourier transform infrared (FTIR) spectra of the prepared INPs, indicating presence of organic compounds from green tea extract.

capping agent and decorate the surface of prepared particles (Ebrahiminezhad et al., 2016a, 2016b). The role of phytochemicals such as ketones, aldehydes, polyphenols, isoverbascosides, and caffeine in the reduction and stabilization of metal nanoparticles repeatedly discussed in the literature (Cruz et al., 2010; Arokiyaraj et al., 2013). The Fe-O stretching vibration from iron oxides produced an indicative band at around 640 cm^{-1} and 450 cm^{-1} (Ebrahiminezhad et al., 2012, 2013). These bonds were not observed in the FTIR spectrum of the prepared particles, which is an indicative for ZVINPs with any iron oxide impurity. Absence of the Fe-O bonds in the FTIR spectra also indicates that phytochemicals in the green tea extract are able to surround the iron particles and provide a perfect protection against oxidation. Similar spectra were reported for both plant mediated synthesized and chemically reduced ZVINPs (Singh et al., 2011; Ebrahiminezhad et al., 2017b).

3.4.3. X-ray spectroscopy

The crystalline structure of the prepared particles was investigated by XRD spectroscopy and the diffraction pattern is presented in Fig. 4. In some reports the tiny diffraction peak at 43° of 2θ degree is considered as characteristic diffraction peak for zero-valent INPs (Kuang et al., 2013; Huang et al., 2014a, 2014b). However, previous studies reported that the INPs synthesized by green tea extracts are amorphous in nature (Njagi et al., 2010; Shahwan et al., 2011; Kuang et al., 2013). The peaks at 32° and 33° of 2θ value are due to mineral complexes (Ebrahiminezhad et al., 2017a). The broad hump peak at around $2\theta = 25°$ is indicating organic compounds from green tea extract that act as capping agent. Presence of the organic compound in the prepared particles was also confirmed by the results from FTIR spectroscopy. These findings are in close agreement with the XRD patterns of zero-valent INPs synthesized using green tea and other plants such as eucalyptus (Kuang et al., 2013; Wang et al., 2014a, 2014b; Truskewycz et al., 2016).

3.4.4. Thermogravimetric analysis

Thermal behavior of the prepared INPs is represented in Fig. 5. At the initial heating range non-bonded water molecules were evaporated and resulted in 3.7% reduction in mass. Heating to 252 °C resulted in evaporation of the residual water and subsequently 30.31% mass loss (Kumar et al., 2010). Decomposition of organic materials makes a peak

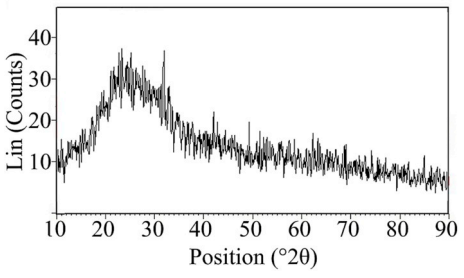

Fig. 4. X-ray powder diffraction (XRD) pattern of the synthesized INPs; no characteristic peak was observed which indicates amorphous structure of the nanoparticles.

at 556.9 °C in the DTG curve. This event resulted in 52.31% reduction in mass which indicates that the weight percentage of biologic coating in the product is about 52% (Kianpour et al., 2016; Ebrahiminezhad et al., 2017b). The percent of biological compound from green tea extract was reported to be 28% for solvothermal synthesized INPs (Karade et al., 2018). Authors introduced reaction time as the indicative factor for the intensity of the formed biological coating. They declared that increase in the reaction time provides more time for growth of nanoparticles and resulted in larger nanoparticles which can possibly reduce the intensity of organic coating (Karade et al., 2018).

3.4.5. Vibrating sample magnetometer

Magnetic properties of the prepared particles were studied using a vibrating sample magnetometer. Fig. 6 shows the results of saturation magnetization analysis at room temperature. Prepared particles showed no hysteresis and the magnetization curve was completely reversible that exhibits a superparamagnetic behavior of prepared nanoparticles. The saturation magnetization value of the synthesized particles was found to be around 80 memu/g. This value is lower than some of the prior reported values for superparamagnetic nanoparticles coated/functionalized with different surfactant molecules. For instance, superparamagnetic Fe_3O_4 nanoparticles coated with green tea polyphenols possessed a high saturation magnetization value equal to 61 emu/g (Singh et al., 2017). But, very low values are not unusual for green synthesized INPs. For instance, synthesis of iron oxide nanoparticles in biochar obtained from the condensed tannin extract from *Acacia mearnsii* revealed very low saturation magnetization value, that were 3.2 and 7.4 memu/g at 300 K and 10 K, respectively (Khan et al., 2015). These low saturation values can be possibly due to diamagnetic properties of biologic capping material and amorphous state of the prepared INPs (Kianpour et al., 2016). Previous studies have indicated that increase in intensity of biological coating by synthesis of nanoparticles in higher concentrations of capping compounds leads to more reduction in saturation magnetization (Ebrahiminezhad et al., 2012, 2013). It has been shown that heating process can significantly increase saturation magnetization values of the green synthesized INPs. Nanoparticles that were synthesized by using zucchini and pomegranate peel extracts were poses 21.4 emu/g and 13.3 emu/g saturation values, respectively. After heat treatment these values were increased to 45.8 emu/g and 38.1 emu/g, respectively (Etemadifar et al., 2018). These findings reveal that magnetic properties of the green synthesized INPs strongly affected by the plant extract phytochemical characteristics and intensity of the organic material that decorate nanoparticles. However, nanostructures with low magnetic saturation values would not be suitable in remediation proposes where magnetic manipulation is required.

3.4.6. Catalytic activity assay

Catalytic potential of the prepared ZVINPs over 6 h is depicted in Fig. 7. Prepared particles were found to be high efficient Fenton catalyst

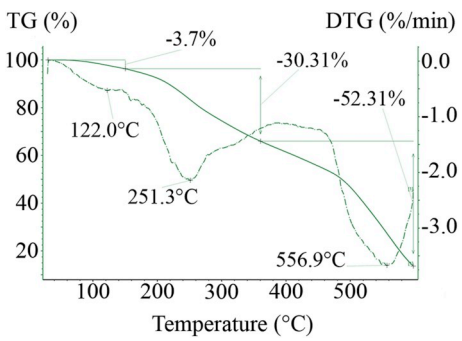

Fig. 5. TGA and DTG curves of the synthesized INPs; the weight loss below 252 °C was due to water evaporation and above 252 °C was due to decomposition of biologic coating.

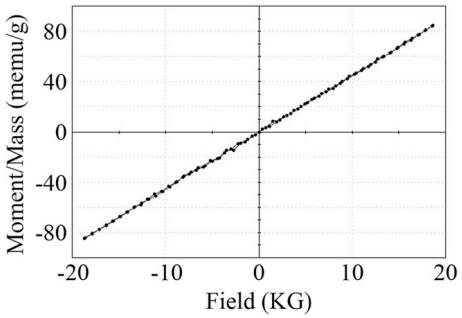

Fig. 6. Magnetization curve of the prepared INPs, magnetization value of the synthesized INPs was measured to be 80 memu/g.

and dye degradation was occurred in a time dependent manner. Similar pattern was also reported for iron nanostructures which synthesized by using green tea extract and other plants (Shahwan et al., 2011; Ebrahiminezhad et al., 2017a). Time dependent pattern is not restricted to a certain catalyst, whereas, increase in the dye removal over time is reported previously for zero-valent INPs, other iron based nanoparticles such as magnetite nanoparticles, and even for iron ions (Youssef et al., 2016; Xu et al., 2018; Taghizadeh et al., 2019). Nanoparticles concentration is another indicative parameter. In this experiment, 1 mg/mL ZVINPs can degrade more than 50% of the initial dye in just 2 h. Similar results were also reported elsewhere. For instance, Xu et al. (2018) have shown that increase in a catalyst concentration which fabricated based on Multi-walled carbon nanotubes (MWCNT) and magnetite nanoparticles resulted in the increase in catalytic potency (Xu et al., 2018). They also showed that addition of MWCNT to the INPs has a synergistic effect on the catalytic activity of nanoparticles.

4. Conclusion

In recent years, plant mediated synthesized ZVINPs are introduced as effective Fenton-like catalyst for environmental remediation purposes. Recent studies indicated green tea as a power full plant for plant mediated synthesis of metallic nanoparticles. In order to achieve highest productivity, DoE and RSM were used successfully for identifying the effective factors and optimal reaction condition for the synthesis of ZVINPs using green tea. The results indicated that the amount of tea extract and concentration of iron precursor are key parameters in green synthesis reaction. The optimal values were identified to be 90% (of reaction volume) and 25 mM (final concentration) for amount of tea extract and iron precursor concentation, respectively. Green tea can efficiently reduce iron ions to zero-valent INPs in a short period. So, reaction time was not identified as effective parameter in nanoparticles production. On the other hand, green tea extract can perform the reduction reaction at room temperature and there is no need to heat the mixture. Phytochemical properties of the green tea along with statistical

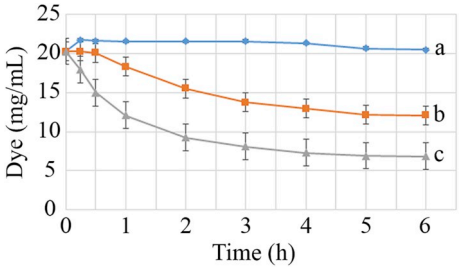

Fig. 7. Catalytic activity of the prepared ZVINPs for methyl orange removal in various concentrations of nanoparticles, 0 mg/mL (a), 0.5 mg/mL (b), and 1 mg/mL (c). (For interpretation of the references to color in this figure legend, the reader is referred to the Web version of this article.)

data which provided by this study can take green tea to the industrial realm for scale up and large-scale production of ZVINPs. Prepared particles were power full Fenton-like catalyst to remove azo dye as a model organic pollutant. The particles were capable to remove more than 50% of the initial dye in just 2 h.

Acknowledgment

This experiment was performed under a collaboration between Fasa University of Medical sciences, Kerman Graduate University of Advanced Technology, Shiraz University of Medical Sciences, and the University of Waikato. Financial supports were received from Fasa University of Medical Sciences and the University of Waikato.

References

Akbari, A., Mohamadzadeh, F., 2012. New method of synthesis of stable zero valent iron nanoparticles (nZVI) by chelating agent diethylene triamine penta acetic acid (DTPA) and removal of radioactive uranium from ground water by using Iron nanoparticle. J. Nanostruct 2, 175–181. http://doi.org/10.7508/JNS.2012.02.004.

Arokiyaraj, S., Saravanan, M., Prakash, N.U., Arasu, M.V., Vijayakumar, B., Vincent, S., 2013. Enhanced antibacterial activity of iron oxide magnetic nanoparticles treated with *Argemone mexicana* L. leaf extract: an in vitro study. Mater. Res. Bull. 48, 3323–3327. http://doi.org/10.1016/j.materresbull.2013.05.059.

Berenjian, A., Mahanama, R., Talbot, A., Biffin, R., Regtop, H., Valtchev, P., Kavanagh, J., Dehghani, F., 2011. Efficient media for high menaquinone-7 production: response surface methodology approach. N. Biotech. 28, 665–672. http://doi.org/10.1016/j.nbt.2011.07.007.

Borja, J.Q., Ngo, M.a.S., Saranglao, C.C., Tiongco, R.P.M., Roque, E.C., Dugos, N.P., 2015. Synthesis of green zero-valent iron using polyphenols from dried green tea extract. J. Eng. Sci. Technol. 10, 22–31.

Cruz, D., Falé, P.L., Mourato, A., Vaz, P.D., Luisa Serralheiro, M., Lino, A.R.L., 2010. Preparation and physicochemical characterization of Ag nanoparticles biosynthesized by *Lippia citriodora* (*Lemon Verbena*). Colloids Surf., B 81, 67–73. http://doi.org/10.1016/j.colsurfb.2010.06.025.

Ebrahiminezhad, A., Bagheri, M., Taghizadeh, S.-M., Berenjian, A., Ghasemi, Y., 2016. Biomimetic synthesis of silver nanoparticles using microalgal secretory carbohydrates as a novel anticancer and antimicrobial. Adv. Nat. Sci. Nanosci. Nanotechnol. 7 https://doi.org/10.1088/2043-6262/7/1/015018. http://doi.org/10.1088/2043-6262/7/1/015018.

Ebrahiminezhad, A., Barzegar, Y., Ghasemi, Y., Berenjian, A., 2016. Green synthesis and characterization of silver nanoparticles using *Alcea rosea* flower extract as a new generation of antimicrobials. Chem. Ind. Chem. Eng. Q. 31–37, 2016. http://doi.org/10.2298/CICEQ150824002E.

Ebrahiminezhad, A., Ghasemi, Y., Rasoul-Amini, S., Barar, J., Davaran, S., 2012. Impact of amino-acid coating on the synthesis and characteristics of iron-oxide nanoparticles (IONs). Bull. Korean Chem. Soc. 33, 3957–3962. http://doi.org/10.5012/bkcs.2012.33.12.3957.

Ebrahiminezhad, A., Ghasemi, Y., Rasoul-Amini, S., Barar, J., Davaran, S., 2013. Preparation of novel magnetic fluorescent nanoparticles using amino acids. Colloids Surf., B 102, 534–539. http://doi.org/10.1016/j.colsurfb.2012.08.046.

Ebrahiminezhad, A., Najafipour, S., Kouhpayeh, A., Berenjian, A., Rasoul-Amini, S., Ghasemi, Y., 2014. Facile fabrication of uniform hollow silica microspheres using a novel biological template. Colloids Surf., B 118, 249–253. http://doi.org/10.1016/j.colsurfb.2014.03.052.

Ebrahiminezhad, A., Rasoul-Amini, S., Ghoshoon, M.B., Ghasemi, Y., 2014. *Chlorella vulgaris*, a novel microalgal source for l-asparaginase production. Biocatal. Agric. Biotechnol. 3, 214–217. http://doi.org/10.1016/j.bcab.2013.10.005.

Ebrahiminezhad, A., Taghizadeh, S., Berenjian, A., Heidaryan Naeini, F., Ghasemi, Y., 2016. Green synthesis of silver nanoparticles capped with natural carbohydrates using *Ephedra intermedia*. Nanosci. Nanotechnol. - Asia 6, 1–9. http://doi.org/10.2174/2210681206666161006165643.

Ebrahiminezhad, A., Taghizadeh, S., Ghasemi, Y., Berenjian, A., 2017. Green synthesized nanoclusters of ultra-small zero valent iron nanoparticles as a novel dye removing material. Sci. Total Environ. 15, 1527–1532. http://doi.org/10.1016/j.scitotenv.2017.10.076Get.

Ebrahiminezhad, A., Zare-Hoseinabadi, A., Berenjian, A., Ghasemi, Y., 2017. Green synthesis and characterization of zero-valent iron nanoparticles using stinging nettle (*Urtica dioica*) leaf extract. Green Process. Synth. 6 https://doi.org/10.1515/gps-2016-0133. http://doi.org/10.1515/gps-2016-0133.

Ebrahiminezhad, A., Zare, M., Kiyanpour, S., Berenjian, A., Niknezhad, S.V., Ghasemi, Y., 2017. Biosynthesis of xanthan gum coated iron nanoparticles by using *Xanthomonas campestris*. IET Nanobiotechnol. 151, 684–691. http://doi.org/10.1049/iet-nbt.2017.0199.

Ebrahiminezhad, A., Zare-Hoseinabadi, A., Sarmah, A.K., Taghizadeh, S., Ghasemi, Y., Berenjian, A., 2017. Plant-mediated synthesis and applications of iron nanoparticles. Mol. Biotechnol. 60 (2), 154–168. https://doi.org/10.1007/s12033-017-0053-4. http://doi.org/10.1007/s12033-017-0053-4, 2017.

Etemadifar, R., Kianvash, A., Arsalani, N., Abouzari-Lotf, E., Hajalilou, A., 2018. Green synthesis of superparamagnetic magnetite nanoparticles: effect of natural surfactant and heat treatment on the magnetic properties. J. Mater. Sci. Mater. Electron. 29, 17144–17153. https://doi.org/10.1021/la0008636.

Ghasemi, Y., Rasoul-Amini, S., Ebrahiminezhad, A., Kazemi, A., Shahbazi, M., Talebnia, N., 2011. Screening and isolation of extracellular protease producing bacteria from the maharloo salt lake. Iran. J. Pharm. Sci. 7, 175–180.

Ghoshoon, M.B., Berenjian, A., Hemmati, S., Dabbagh, F., Karimi, Z., Negahdaripour, M., Ghasemi, Y., 2015. Extracellular production of recombinant L-Asparaginase II in *Escherichia coli*: medium optimization using response surface methodology. Int. J. Pept. Res. Ther. 21, 487–495. http://doi.org/10.1007/s10989-015-9476-6.

Grundl, T., Delwiche, J., 1993. Kinetics of ferric oxyhydroxide precipitation. J. Contam. Hydrol. 14, 71–87. http://doi.org/10.1016/0169-7722(93)90042-Q.

Gudelj, I., Hrenović, J., Dragičević, T., Delaš, F., Gudelj, H., 2011. Azo dyes, their environmental effects, and defining a strategy for their biodegradation and detoxification. Arh. Hig. Rada. Toksiko. 62, 91–101. http://doi.org/10.2478/10004-1254-62-2011-2063.

Huang, L., Luo, F., Chen, Z., Megharaj, M., Naidu, R., 2015. Green synthesized conditions impacting on the reactivity of Fe NPs for the degradation of malachite green. Spectrochim. Acta 137, 154–159. http://doi.org/10.1016/j.saa.2014.08.116.

Huang, L., Weng, X., Chen, Z., Megharaj, M., Naidu, R., 2014. Green synthesis of iron nanoparticles by various tea extracts: comparative study of the reactivity. Spectrochim. Acta 130, 295–301. http://doi.org/10.1016/j.saa.2014.04.037.

Huang, L., Weng, X., Chen, Z., Megharaj, M., Naidu, R., 2014. Synthesis of iron-based nanoparticles using oolong tea extract for the degradation of malachite green. Spectrochim. Acta 117, 801–804. http://doi.org/10.1016/j.saa.2013.09.054.

Jiang, J., Pi, J., Cai, J., 2018. The advancing of zinc oxide nanoparticles for biomedical applications. Bioinorgan. Chem. Appl. 1062562 https://doi.org/10.1155/2018/1062562. eCollection 2018, 2018. http://doi.org/10.1155/2018/1062562.

Karade, V., Dongale, T., Sahoo, S.C., Kollu, P., Chougale, A., Patil, P., Patil, P., 2018. Effect of reaction time on structural and magnetic properties of green-synthesized magnetic nanoparticles. J. Phys. Chem. Solids 120, 161–166. http://doi.org/10.1016/j.jpcs.2018.04.040.

Khan, M., Mangrich, A., Schultz, J., Grasel, F., Mattoso, N., Mosca, D., 2015. Green chemistry preparation of superparamagnetic nanoparticles containing Fe_3O_4 cores in biochar. J. Anal. Appl. Pyrolysis 116, 42–48. http://doi.org/10.1016/j.jaap.2015.10.008.

Khoo, K.S., Lee, S.Y., Ooi, C.W., Fu, X., Miao, X., Ling, T.C., Show, P.L., 2019. Recent advances in biorefinery of astaxanthin from Haematococcus pluvialis. Bioresour. Technol. 288 (121606) https://doi.org/10.1016/j.biortech.2019.121606, 121606. http://doi.org/10.1016/j.biortech.2019.121606.

Kianpour, S., Ebrahiminezhad, A., Mohkam, M., Tamaddon, A.M., Dehshahri, A., Heidari, R., Ghasemi, Y., 2016. Physicochemical and biological characteristics of the nanostructured polysaccharide-iron hydrogel produced by microorganism *Klebsiella oxytoca*. J. Basic Microbiol. 132–140, 2016. http://doi.org/10.1002/jobm.201600417.

Kianpour, S., Ebrahiminezhad, A., Negahdaripour, M., Mohkam, M., Mohammadi, F., Niknezhad, S., Ghasemi, Y., 2018. Characterization of biogenic Fe (III)-binding exopolysaccharide nanoparticles produced by *Ralstonia* sp. SK03. Biotechnol. Prog. 34, 1167–1176. http://doi.org/10.1002/btpr.2660.

Kuang, Y., Wang, Q., Chen, Z., Megharaj, M., Naidu, R., 2013. Heterogeneous Fenton-like oxidation of monochlorobenzene using green synthesis of iron nanoparticles. J. Colloid Interface Sci. 410, 67–73. http://doi.org/10.1016/j.jcis.2013.08.020.

Kumar, A., Singhal, A., 2007. Synthesis of colloidal β-Fe_2O_3 nanostructures—influence of addition of Co^{2+} on their morphology and magnetic behavior. Nanotechnology 18. http://doi.org/10.1088/0957-4484/18/47/475703.

Kumar, R., Inbaraj, B.S., Chen, B., 2010. Surface modification of superparamagnetic iron nanoparticles with calcium salt of poly (γ-glutamic acid) as coating material. Mater. Res. Bull. 45, 1603–1607. http://doi.org/10.1016/j.materresbull.2010.07.017.

Lahann, J., 2008. Environmental nanotechnology: nanomaterials clean up. Nat. Nanotechnol. 3. http://doi.org/10.1038/nnano.2008.143.

Li, L., Hu, J., Shi, X., Fan, M., Luo, J., Wei, X., 2016. Nanoscale zero-valent metals: a review of synthesis, characterization, and applications to environmental remediation. Environ. Sci. Pollut. Res. 23, 17880–17900. http://doi.org/10.1007/s11356-016-6626-0.

Li, X.-Q., Elliott, D.W., Zhang, W.-X., 2006. Zero-valent iron nanoparticles for abatement of environmental pollutants: materials and engineering aspects. Crit. Rev. Solid State 31, 111–122. http://doi.org/10.1080/10408430601057611.

López-Sánchez, J., Muñoz-Noval, A., Serrano, A., Abuín, M., De La Figuera, J., Marco, J., Pérez, L., Carmona, N., De La Fuente, O.R., 2016. Growth, structure and magnetism of ε-Fe_2O_3 in nanoparticle form. RSC Adv. 6, 46380–46387. http://doi.org/10.1039/C6RA01912A.

Lu, H., Wang, J., Stoller, M., Wang, T., Bao, Y., Hao, H., 2016. An overview of nanomaterials for water and wastewater treatment. Advances in Materials Science and Engineering 4964828. https://doi.org/10.1155/2016/4964828, 2016.

Machado, S., Pinto, S., Grosso, J., Nouws, H., Albergaria, J.T., Delerue-Matos, C., 2013. Green production of zero-valent iron nanoparticles using tree leaf extracts. Sci. Total Environ. 445, 1–8. http://doi.org/10.1016/j.scitotenv.2012.12.033.

Muthukumar, H., Matheswaran, M., 2015. *Amaranthus spinosus* leaf extract mediated FeO nanoparticles: physicochemical traits, Photocatalytic and Antioxidant activity. ACS Sustain. Chem. Eng. 3, 3149–3156. http://doi.org/10.1021/acssuschemeng.5b00722.

Nagajyothi, P., Pandurangan, M., Kim, D.H., Sreekanth, T., Shim, J., 2017. Green synthesis of iron oxide nanoparticles and their catalytic and in vitro anticancer activities. J. Clust. Sci. 28, 245–257. http://doi.org/10.1007/s10876-016-1082-z.

Njagi, E.C., Huang, H., Stafford, L., Genuino, H., Galindo, H.M., Collins, J.B., Hoag, G.E., Suib, S.L., 2010. Biosynthesis of iron and silver nanoparticles at room temperature

using aqueous sorghum bran extracts. Langmuir 27, 264–271. http://doi.org/10.1021/la103190n.
Ohkoshi, S.-I., Namai, A., Yamaoka, T., Yoshikiyo, M., Imoto, K., Nasu, T., Anan, S., Umeta, Y., Nakagawa, K., Tokoro, H., 2016. Mesoscopic bar magnet based on ε-Fe_2O_3 hard ferrite. Sci. Rep. 6. http://doi.org/10.1038/srep27212.
Plachtová, P., MedŘíková, Z., ZboŘIl, R., TučEk, J.I., Varma, R.S., MaršáLek, B., 2018. Iron and iron oxide nanoparticles synthesized with green tea extract: differences in ecotoxicological profile and ability to degrade malachite green. ACS Sustain. Chem. Eng. 6, 8679–8687. http://doi.org/10.1021/acssuschemeng.8b00986.
Rajiv, P., Bavadharani, B., Kumar, M.N., Vanathi, P., 2017. Synthesis and characterization of biogenic iron oxide nanoparticles using green chemistry approach and evaluating their biological activities. Biocatal. Agric. Biotechnol. 12, 45–49. http://doi.org/10.1016/j.bcab.2017.08.015.
Ranmadugala, D., Ebrahiminezhad, A., Manley-Harris, M., Ghasemi, Y., Berenjian, A., 2017. Reduced biofilm formation in Menaquinone-7 production process by optimizing the composition of the cultivation medium. Trends Pharmacol. Sci. 3, 245–254. http://doi.org/10.1111/tips.v3i4.153.
Rezaei, F., Vione, D., 2018. Effect of pH on zero valent iron performance in heterogeneous fenton and fenton-like processes: a review. Molecules 23, 3127.
Seifan, M., Ebrahiminezhad, A., Ghasemi, Y., Berenjian, A., 2019. Microbial calcium carbonate precipitation with high affinity to fill the concrete pore space: nanobiotechnological approach. Bioproc. Biosyst. Eng. 42, 37–46. http://doi.org/10.1007/s00449-018-2011-3.
Shahwan, T., Sirriah, S.A., Nairat, M., Boyacı, E., Eroğlu, A.E., Scott, T.B., Hallam, K.R., 2011. Green synthesis of iron nanoparticles and their application as a Fenton-like catalyst for the degradation of aqueous cationic and anionic dyes. Chem. Eng. J. 172, 258–266. http://doi.org/10.1016/j.cej.2011.05.103.
Singh, K., Senapati, K., Sarma, K., 2017. Synthesis of superparamagnetic Fe_3O_4 nanoparticles coated with green tea polyphenols and their use for removal of dye pollutant from aqueous solution. J. Environ. Chem. Eng. 5, 2214–2221. http://doi.org/10.1016/j.jece.2017.04.022.
Singh, R., Misra, V., Singh, R.P., 2011. Synthesis, characterization and role of zero-valent iron nanoparticle in removal of hexavalent chromium from chromium-spiked soil. J. Nanoparticle Res. 13, 4063–4073. http://doi.org/10.1007/s11051-011-0350-y.
Sulaiman, G.M., Tawfeeq, A.T., Naji, A.S., 2018. Biosynthesis, characterization of magnetic iron oxide nanoparticles and evaluations of the cytotoxicity and DNA damage of human breast carcinoma cell lines. Artif. Cell Nanomed. Biotechnol. 46, 1215–1229. http://doi.org/10.1080/21691401.2017.1366335.
Taghizadeh, S.-M., Berenjian, A., Taghizadeh, S., Ghasemi, Y., Taherpour, A., Sarmah, A. K., Ebrahiminezhad, A., 2019. One-put green synthesis of multifunctional silver iron core-shell nanostructure with antimicrobial and catalytic properties. Ind. Crops Prod. 130, 230–236. http://doi.org/10.1016/j.indcrop.2018.12.085.
Tatarko, M., Tricker, J., Andrzejewski, K., Bumpus, J.A., Rhoads, H., 1999. Remediation of water contaminated with an azo dye: an undergraduate laboratory experiment utilizing an inexpensive photocatalytic reactor. J. Chem. Educ. 76. http://doi.org/10.1021/ed076p1680.
Torrey, J.D., Killgore, J.P., Bedford, N.M., Greenlee, L.F., 2015. Oxidation behavior of zero-valent iron nanoparticles in mixed matrix water purification membranes. Environ. Sci.: Water Res. Technol. 1, 146–152.
Truskewycz, A., Shukla, R., Ball, A.S., 2016. Iron nanoparticles synthesized using green tea extracts for the fenton-like degradation of concentrated dye mixtures at elevated temperatures. J. Environ. Chem. Eng. 4, 4409–4417. http://doi.org/10.1016/j.jece.2016.10.008.
Tuček, J., Machala, L., Ono, S., Namai, A., Yoshikiyo, M., Imoto, K., Tokoro, H., Ohkoshi, S.-I., Zbořil, R., 2015. Zeta-Fe_2O_3–A new stable polymorph in iron (III) oxide family. Sci. Rep. 5. http://doi.org/10.1038/srep15091.
Tucek, J., Zboril, R., Namai, A., Ohkoshi, S.-I., 2010. ε-Fe_2O_3: an advanced nanomaterial exhibiting giant coercive field, millimeter-wave ferromagnetic resonance, and magnetoelectric coupling. Chem. Mater. 22, 6483–6505. http://doi.org/10.1021/cm101967h.
Wang, T., Jin, X., Chen, Z., Megharaj, M., Naidu, R., 2014. Green synthesis of Fe nanoparticles using eucalyptus leaf extracts for treatment of eutrophic wastewater. Sci. Total Environ. 466, 210–213. http://doi.org/10.1016/j.scitotenv.2013.07.022.
Wang, T., Lin, J., Chen, Z., Megharaj, M., Naidu, R., 2014. Green synthesized iron nanoparticles by green tea and eucalyptus leaves extracts used for removal of nitrate in aqueous solution. J. Clean. Prod. 83, 413–419. http://doi.org/10.1016/j.jclepro.2014.07.006.
Xiao, Z., Yuan, M., Yang, B., Liu, Z., Huang, J., Sun, D., 2016. Plant-mediated synthesis of highly active iron nanoparticles for Cr (VI) removal: investigation of the leading biomolecules. Chemosphere 150, 357–364. http://doi.org/10.1016/j.chemosphere.2016.02.056.
Xu, H.-Y., Wang, Y., Shi, T.-N., Zhao, H., Tan, Q., Zhao, B.-C., He, X.-L., Qi, S.-Y., 2018. Heterogeneous Fenton-like discoloration of methyl orange using Fe_3O_4/MWCNTs as catalyst: combination mechanism and affecting parameters. Front. Mater. Sci. 12, 21–33. http://doi.org/10.1007/s11706-018-0408-1.
Yang, J., Hou, B., Wang, J., Tian, B., Bi, J., Wang, N., Li, X., Huang, X., 2019. Nanomaterials for the removal of heavy metals from wastewater. Nanomaterials 9, 424.
Yew, G.Y., Lee, S.Y., Show, P.L., Tao, Y., Law, C.L., Nguyen, T.T.C., Chang, J.-S., 2019. Recent advances in algae biodiesel production: from upstream cultivation to downstream processing. Bioresource Technology Reports 7, 100227.
Youssef, N.A., Shaban, S.A., Ibrahim, F.A., Mahmoud, A.S., 2016. Degradation of methyl orange using Fenton catalytic reaction. Egypt. J. Perol. 25, 317–321. http://doi.org/10.1016/j.ejpe.2015.07.017.
Yuvakkumar, R., Elango, V., Rajendran, V., Kannan, N., 2011. Preparation and characterization of zero valent iron nanoparticles. Dig. J. Nanomater. Biostruct. 6, 1771–1776.